TransNav
http://www.transnav.eu
the International Journal
on Marine Navigation
and Safety of Sea Transportation
Volume 14
Number 3
September 2020
DOI: 10.12716/1001.14.03.16

Mathematical Models of a Pneumatic Cascade and Pneumatic Membrane Actuator Described with a Fractional Calculus

M. Luft, Z. Łukasik & D. Pietruszczak
Kazimierz Pulaski University of Technology and Humanities in Radom, Radom, Poland

ABSTRACT: The paper presents the analysis of dynamic properties of pneumatic systems such as: cascade connection of membrane pressure transmitters and a pneumatic membrane actuator by means of differential equations of integer and non-integer order. The analyzed systems were described from the time perspective by means of step response, and in terms of frequency with the help of the Bode plot, i.e. logarithmic magnitude and phase responses.
Each response was determined using differential equations of non-integer order.
To determine the responses, the interactive Simulink package was an irreplaceable programming tool built on the basis of the MATLAB program, which enables the analysis and synthesis of continuous dynamic systems.

1 INTRODUCTION

The article presents the mathematical analysis of the pneumatic cascade and the pneumatic membrane actuator described with the differential calculus of non-integer orders (*Fractional calculus*) [1], [2], [3], [5], [6], [7], [8], [9], [10], [13] and [15].

Differential equations of integer and non-integer order were introduced and became the basis for deriving equations describing time characteristics (pulse and step) and frequency characteristics (logarithmic amplitude and phase characteristics) for each tested pneumatic system [11]. Next, simulations of derived equations were performed using Microsoft Excel and MATLAB & Simulink software, obtaining time and frequency characteristics of the tested systems for integer and non-integer orders [12], [14], [16], [17] and [18].

2 MATHEMATICAL MODEL OF A PNEUMATIC CASCADE DESCRIBED WITH A FRACTIONAL CALCULUS

Fig. 1 shows the diagram of the analyzed pneumatic cascade:

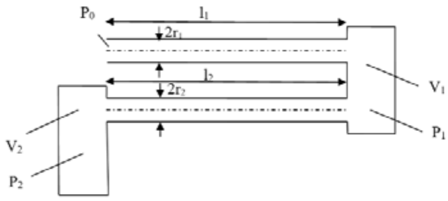

Figure 1. Diagram of a two-chamber pneumatic cascade [11]

Fig. 2 shows a block diagram of a two-chamber pneumatic cascade:

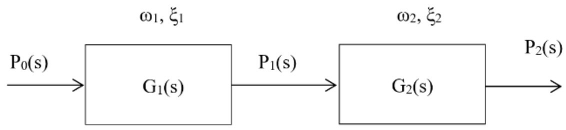

Figure 2. Block diagram of a two-chamber pneumatic cascade [11]

Assuming the linearity of the model, the equation describing the dynamics of the diaphragm pressure transmitter can be written in the form of a system of differential equations:

$$\frac{d^2 p_1(t)}{dt^2} + 2\xi_1\omega_1 \frac{dp_1(t)}{dt} + \omega_1^2 p_1(t) = \omega_1^2 p_0(t) \tag{1a}$$

$$\frac{d^2 p_2(t)}{dt^2} + 2\xi_2\omega_2 \frac{dp_2(t)}{dt} + \omega_2^2 p(t) = \omega_2^2 p_1(t) \tag{1b}$$

where:

$\omega_{1,2}\left(rad/s\right)$ - the pulsatance of another elementary pneumatic system,

$\xi_{1,2} < 1$ - the damping ratio of another elementary pneumatic system included in the pneumatic cascade.

$$\omega_{1,2} = \frac{1}{\sqrt{L_{p1,p2} C_{p1,p2}}} = \sqrt{\frac{3\pi r_{1,2}^2 c^2}{4 l_{1,2} V_{1,2}}} \tag{2a}$$

$$\zeta_{1,2} = \frac{L_{p1,p2} C_{p1,p2} \omega_{1,2}}{2} = 2\frac{\eta\sqrt{\frac{3 l_{1,2} V_{1,2}}{\pi}}}{r_{1,2}\rho c} = 2\sqrt{\frac{3\eta^2 l_{1,2} V_{1,2}}{\pi r_{1,2}^2 \rho^2 c^2}} \tag{2b}$$

wherein:

$C_p\left[Ns^2 m^{-5}\right]$ - pneumatic capacity in another element of the pneumatic system;

$L_p\left[m^3 N^{-1}\right]$ - pneumatic induction in another element of the pneumatic system;

$R_p\left[Nsm^{-5}\right]$ - flow resistance in another element of the pneumatic system;

$V\left[m^3\right]$ - volume of another transducer chamber,

$c\left[m/s\right]$ - speed of sound in the gas filling the system;

$l\left[m\right]$ - length of another inlet pipe;

$r\left[m\right]$ - radius of another inlet tube;

$\rho\left[kgm^{-3}\right]$ - gas density;

$\eta\left[kgm^{-1}s^{-1}\right]$ - dynamic viscosity.

Equations (1) written with the help of fractional calculus take the following form:

$$\begin{aligned} {}_0^{RL}D_t^{2v} p_1(t) + 2\xi_1\omega_1 \, {}_0^{RL}D_t^{v} p_1(t) + \omega_1^2 p_1(t) &= \omega_1^2 p_0(t) \\ {}_0^{RL}D_t^{2v} p_2(t) + 2\xi_2\omega_2 \, {}_0^{RL}D_t^{v} p_2(t) + \omega_2^2 p_2(t) &= \omega_2^2 p_1(t) \end{aligned} \tag{3}$$

where: $v > 0$.

Using the Laplace transform to equation (3), for zero initial conditions, we obtain:

$$\begin{aligned} \left(s^{2v} + 2\xi_1\omega_1 s^v + \omega_1^2\right) p_1(s) &= \omega_1^2 p_0(s) \\ \left(s^{2v} + 2\xi_2\omega_2 s^v + \omega_2^2\right) p_2(s) &= \omega_2^2 p_1(s) \end{aligned} \tag{4}$$

Thus the transfer function of non-integer order of the analyzed pneumatic system is obtained:

$$\begin{aligned} G_1^{(v)}(s) &= \frac{p_1(s)}{p_0(s)} = \frac{\omega_1^2}{s^{2v} + 2\xi_1\omega_1 s^v + \omega_1^2} \\ G_2^{(v)}(s) &= \frac{p_2(s)}{p_1(s)} = \frac{\omega_2^2}{s^{2v} + 2\xi_2\omega_2 s^v + \omega_2^2} \end{aligned} \tag{5}$$

The transfer function of the analyzed system takes the form:

$$\begin{aligned} G^{(v)}(s) &= \frac{p_2(s)}{p_0(s)} = G_1^{(v)}(s) G_2^{(v)}(s) \\ G^{(v)}(s) &= \frac{\omega_1^2\omega_2^2}{s^{4v} + \left(2\xi_1\omega_1 + 2\xi_2\omega_2\right)s^{3v} + \left(\omega_1^2 + 4\xi_1\xi_2\omega_1\omega_2 + \omega_2^2\right)s^{2v} + \left(2\xi_1\omega_1\omega_2^2 + 2\xi_2\omega_1^2\omega_2\right)s^v + \omega_1^2\omega_2^2} \end{aligned} \tag{6}$$

For the formula (6), we obtain the spectral transfer function of the tested transducer:

$$G^v(j\omega) = \frac{\omega_1^2\omega_2^2}{\begin{aligned} &\omega^{4v}\left[\cos(2\pi v) + j\sin(2\pi v)\right] + \left(2\xi_1\omega_1 + 2\xi_2\omega_2\right)\omega^{3v}\left[\cos\left(\frac{3\pi v}{2}\right) + j\sin\left(\frac{3\pi v}{2}\right)\right] + \\ &\left(\omega_1^2 + 4\xi_1\xi_2\omega_1\omega_2 + \omega_2^2\right)\omega^{2v}\left[\cos(\pi v) + j\sin(\pi v)\right] + \\ &+\left(2\xi_1\omega_1\omega_2^2 + 2\xi_2\omega_1^2\omega_2\right)\omega^v\left[\cos\left(\frac{\pi v}{2}\right) + j\sin\left(\frac{\pi v}{2}\right)\right] + \omega_1^2\omega_2^2 \end{aligned}} \tag{7}$$

By making elementary transformations, the real and imaginary part of the spectral transfer function is calculated:

$$G^{(v)}(j\omega) = P^{(v)}(\omega) + jQ^{(v)}(\omega) \tag{8}$$

where:

$$P^v(j\omega) = \frac{\begin{aligned} &\omega_1^2\omega_2^2\left[\omega^{4v}\cos(2\pi v) + 2\xi_1\omega_1\omega^{3v}\cos\left(\frac{3\pi v}{2}\right) + 2\xi_2\omega_2\omega^{3v}\cos\left(\frac{3\pi v}{2}\right) + \right. \\ &\omega_1^2\omega^{2v}\cos(\pi v) + 4\xi_1\xi_2\omega_1\omega_2\omega^{2v}\cos(\pi v) + \omega_2^2\omega^{2v}\cos(\pi v) + 2\xi_1\omega_1\omega_2^2\omega^v\cos\left(\frac{\pi v}{2}\right) + \\ &\left. 2\xi_2\omega_1^2\omega_2\omega^v\cos\left(\frac{\pi v}{2}\right) + \omega_1^2\omega_2^2\right] \end{aligned}}{\begin{aligned} &\left[\omega^{4v}\cos(2\pi v) + 2\xi_1\omega_1\omega^{3v}\cos\left(\frac{3\pi v}{2}\right) + 2\xi_2\omega_2\omega^{3v}\cos\left(\frac{3\pi v}{2}\right) + \omega_1^2\omega^{2v}\cos(\pi v) + \right. \\ &4\xi_1\xi_2\omega_1\omega_2\omega^{2v}\cos(\pi v) + \omega_2^2\omega^{2v}\cos(\pi v) + 2\xi_1\omega_1\omega_2^2\omega^v\cos\left(\frac{\pi v}{2}\right) + 2\xi_2\omega_1^2\omega_2\omega^v\cos\left(\frac{\pi v}{2}\right) + \\ &\left.\omega_1^2\omega_2^2\right]^2 + \left[\omega^{4v}\sin(2\pi v) + 2\xi_1\omega_1\omega^{3v}\sin\left(\frac{3\pi v}{2}\right) + 2\xi_2\omega_2\omega^{3v}\sin\left(\frac{3\pi v}{2}\right) + \omega_1^2\omega^{2v}\sin(\pi v) + \right. \\ &\left. 4\xi_1\xi_2\omega_1\omega_2\omega^{2v}\sin(\pi v) + \omega_2^2\omega^{2v}\sin(\pi v) + 2\xi_1\omega_1\omega_2^2\omega^v\sin\left(\frac{\pi v}{2}\right) + 2\xi_2\omega_1^2\omega_2\omega^v\sin\left(\frac{\pi v}{2}\right)\right]^2 \end{aligned}} \tag{9}$$

$$
Q^{v}(j\omega)=\frac{\omega_1^2\omega_2^2\left[\omega^{4v}\sin(2\pi v)+2\xi_1\omega_1\omega^{3v}\sin\left(\frac{3\pi v}{2}\right)+2\xi_2\omega_2\omega^{3v}\sin\left(\frac{3\pi v}{2}\right)+\omega_1^2\omega^{2v}\sin(\pi v)+4\xi_1\xi_2\omega_1\omega_2\omega^{2v}\sin(\pi v)+\omega_2^2\omega^{2v}\sin(\pi v)+2\xi_1\omega_1\omega_2^2\omega^{v}\sin\left(\frac{\pi v}{2}\right)+2\xi_2\omega_1^2\omega_2\omega^{v}\sin\left(\frac{\pi v}{2}\right)\right]}{\left[\omega^{4v}\cos(2\pi v)+2\xi_1\omega_1\omega^{3v}\cos\left(\frac{3\pi v}{2}\right)+2\xi_2\omega_2\omega^{3v}\cos\left(\frac{3\pi v}{2}\right)+\omega_1^2\omega^{2v}\cos(\pi v)+4\xi_1\xi_2\omega_1\omega_2\omega^{2v}\cos(\pi v)+\omega_2^2\omega^{2v}\cos(\pi v)+2\xi_1\omega_1\omega_2^2\omega^{v}\cos\left(\frac{\pi v}{2}\right)+2\xi_2\omega_1^2\omega_2\omega^{v}\cos\left(\frac{\pi v}{2}\right)+\omega_1^2\omega_2^2\right]^2+\left[\omega^{4v}\sin(2\pi v)+2\xi_1\omega_1\omega^{3v}\sin\left(\frac{3\pi v}{2}\right)+2\xi_2\omega_2\omega^{3v}\sin\left(\frac{3\pi v}{2}\right)+\omega_1^2\omega^{2v}\sin(\pi v)+4\xi_1\xi_2\omega_1\omega_2\omega^{2v}\sin(\pi v)+\omega_2^2\omega^{2v}\sin(\pi v)+2\xi_1\omega_1\omega_2^2\omega^{v}\sin\left(\frac{\pi v}{2}\right)+2\xi_2\omega_1^2\omega_2\omega^{v}\sin\left(\frac{\pi v}{2}\right)\right]^2} \tag{10}
$$

Knowing the real and imaginary part of the spectral transfer function of the transducer, one can determine the equation describing the logarithmic amplitude step:

$$
L^{(v)}(\omega)=20log\sqrt{\left[P^{(v)}(\omega)\right]^2+\left[Q^{(v)}(\omega)\right]^2} \tag{11}
$$

and the equation describing the logarithmic phase step:

$$
\varphi^{(v)}(\omega)=arctg\left[\frac{Q^{v}(\omega)}{P^{v}(\omega)}\right]= -arctg\left[\frac{\omega^{4v}\sin(2\pi v)+2\xi_1\omega_1\omega^{3v}\sin\left(\frac{3\pi v}{2}\right)+2\xi_2\omega_2\omega^{3v}\sin\left(\frac{3\pi v}{2}\right)+\omega_1^2\omega^{2v}\sin(\pi v)+4\xi_1\xi_2\omega_1\omega_2\omega^{2v}\sin(\pi v)+\omega_2^2\omega^{2v}\sin(\pi v)+2\xi_1\omega_1\omega_2^2\omega^{v}\sin\left(\frac{\pi v}{2}\right)+2\xi_2\omega_1^2\omega_2\omega^{v}\sin\left(\frac{\pi v}{2}\right)}{\omega^{4v}\cos(2\pi v)+2\xi_1\omega_1\omega^{3v}\cos\left(\frac{3\pi v}{2}\right)+2\xi_2\omega_2\omega^{3v}\cos\left(\frac{3\pi v}{2}\right)+\omega_1^2\omega^{2v}\cos(\pi v)+4\xi_1\xi_2\omega_1\omega_2\omega^{2v}\cos(\pi v)+\omega_2^2\omega^{2v}\cos(\pi v)+2\xi_1\omega_1\omega_2^2\omega^{v}\cos\left(\frac{\pi v}{2}\right)+2\xi_2\omega_1^2\omega_2\omega^{v}\cos\left(\frac{\pi v}{2}\right)+\omega_1^2\omega_2^2}\right] \tag{12}
$$

Using the program written in the MATLAB environment, which was used for conducting the simulations of the equations describing the Bode plot (11) and (12) of the membrane pressure transducer, a response in the form of plots of logarithmic magnitude and phase of the analyzed pneumatic cascade was obtained. The plots are presented in Fig. 3 and Fig. 4.

The determined frequency response (Fig. 3 and Fig. 4) correctly reflect the dynamics of the model. For the parameter $v=1$, the logarithmic amplitude response (Fig. 3) and phase response (Fig. 4) coincide with the known responses of the 4th order oscillation units. From the amplitude response (Fig. 3), one can read the gain decrease, which is $-80dB/dek$, and from the phase response (Fig. 4), the phase shift $\varphi=-2\pi$ for the parameter $v=1$, as it is in the classic oscillation section of the 4th order.

The analysis of frequency responses (Fig. 3 and Fig. 4) shows that the resonant pulsation depends on the parameter v, and hence on the order of the differential, in the differential equation describing the studied system. By reducing the order, the resonant pulsation increases. Hence, the smaller the phase shift of the system is, the smaller the order of the differential.

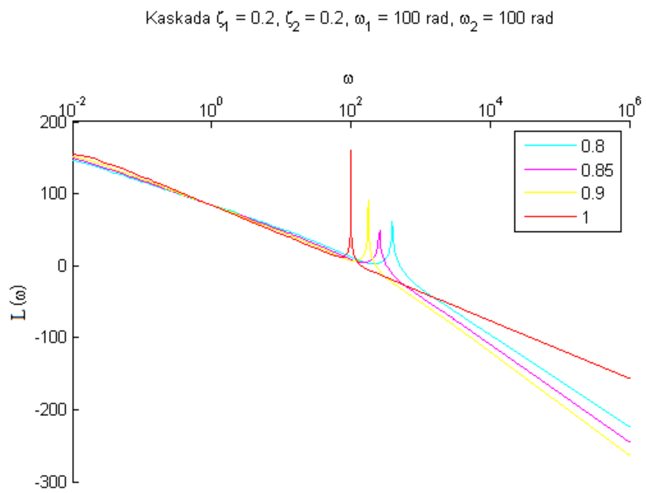

Figure 3. Logarithmic amplitude response of a pneumatic cascade described by means of differential equation with fractional derivatives of non-integer orders for the parameter v in the range (0.8-1.2) [authors' own elaboration]

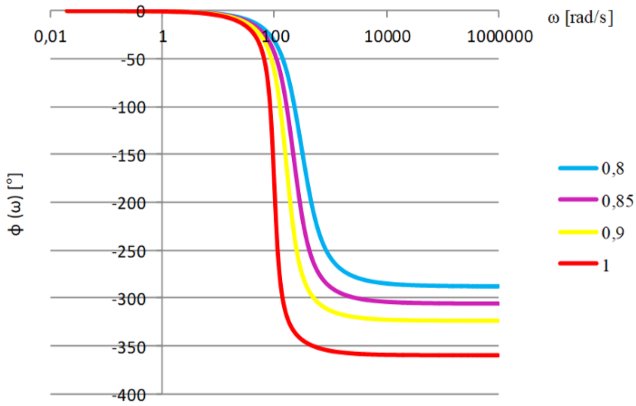

Figure 4. Logarithmic phase response of a pneumatic cascade described by means of differential equation with fractional derivatives of non-integer orders for the parameter v in the range (0.8-1.2) [authors' own elaboration]

3 MATHEMATICAL MODEL OF A PNEUMATIC MEMBRANE ACTUATOR DESCRIBED WITH A FRACTIONAL CALCULUS

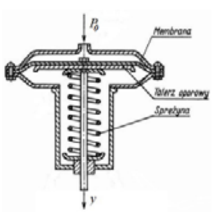

Figure 5. Pneumatic membrane actuator [11]
(*Membrana* - Membrane, *Talerz oporowy* - Retaining plate, *Sprężyna* - Spring)

Based on Newton's laws, we can write:

$$
m\frac{d^2y(t)}{dt^2}+R\frac{dy(t)}{dt}+Cy(t)=Ap_0(t) \tag{13}
$$

where:

$p_0[Pa]$ - inlet pressure (forcing);

$A[m^2]$ - active surface of the membrane;

$m[kg]$ - mass of the mobile system;

$C[Nm^{-1}]$ - spring stiffness coefficient;

$R[Nsm^{-1}]$ - viscous friction coefficient;

$y[m]$ - displacement of the actuator stem.

If the damping of the system $\xi<1$, then $R<2\sqrt{mC}$.

Generalizing the equation (13), we get:

$$m_0^{RL}D_t^{2v}y(t)+R_0^{RL}D_t^v y(t)+Cy(t)=Ap_0(t) \tag{14}$$

where: $v>0$.

Applying the Laplace transform, assuming zero initial conditions, for a fractional derivative of non-integer order defined by Riemann - Liouville, we obtain:

$$mY(s)\left(s^{2v}+\frac{R}{m}s^v+\frac{C}{m}\right)=Ap_0(s) \tag{15}$$

Thus the transfer function of non-integer order of the membrane pneumatic actuator is obtained:

$$G^{(v)}(s)=\frac{Y(s)}{P_0(s)}=\frac{\frac{A}{m}}{s^{2v}+\frac{R}{m}s^v+\frac{C}{m}} \tag{16}$$

In order to conduct a simulation, the data of a pneumatic membrane actuator of the GMP brake T16 were used:

A - effective membrane surface: for r = 50mm (diameter = 100mm) A = 0.00785 m2;

m - mass of the mobile system (membrane and plunger); m = 0.12 + 0.2 = 0.32 kg;

C - spring stiffness coefficient; C = 1000N / m

R - viscous friction coefficient (resistance to movement of moving parts) - R = 0,5Ns / m.

By substituting the above data for the equation (16), the transfer function of the analyzed pneumatic actuator was obtained:

$$G^{(v)}(s)=\frac{Y(s)}{P_0(s)}=\frac{0,025}{s^{2v}+1,56s^v+3125} \tag{17}$$

The quantifier of the non-integer transfer function has two complex roots. Therefore, you get:

$$\left.\begin{matrix}g^{(v)}(t)\\h^{(v)}(t)\end{matrix}\right\}=0,025\sum_{k=0}^{\infty}\frac{(-1)^k}{k!}(3125)^k\,\varepsilon_k\left(t,-1,56;v,2v+vk+\begin{Bmatrix}0\\1\end{Bmatrix}\right) \tag{18}$$

For the equation (8), you get the equations describing the impulse and step response of the incomplete order of the tested pneumatic actuator in the form of:

$$\left.\begin{matrix}g^{(v)}(t)\\h^{(v)}(t)\end{matrix}\right\}=0,025\sum_{k=0}^{\infty}\frac{(-1)^k}{k!}(3125)^k\begin{Bmatrix}t^{2v(k+1)-1}E_{v,2v+vk}^{(k)}\left(-1,56t^v\right)\\t^{2v(k+1)}E_{v,2v+vk}^{(k)}\left(-1,56t^v\right)\end{Bmatrix} \tag{19}$$

whereas the function $E_{\alpha,\beta}^{(k)}(z)$ is a special type of Mittag-Leffler function.

By conducting a simulation of the pneumatic transducer, a pulse and unit jump signal was applied thus receiving the impulse and step response shown in Figure 6 and Figure 7.

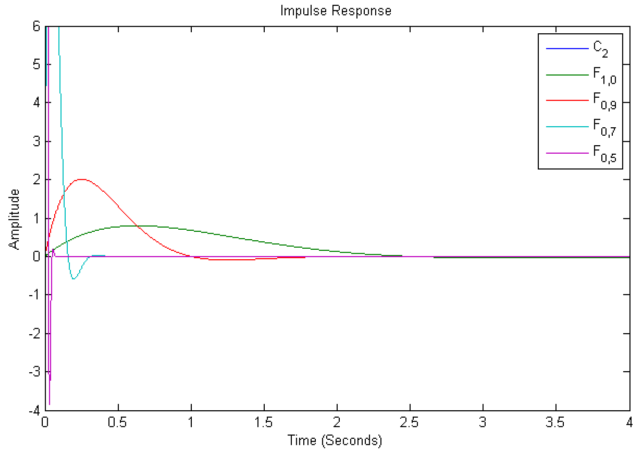

Figure 6. Impulse response of a pneumatic actuator described with integer and non-integer order: $F_{0,5}$ - for $v=0,5$, $F_{0,7}$ - for $v=0,7$, $F_{0,9}$ - for $v=0,9$, $F_{1,0}$ - for $v=1$, C_2 - classic model (integer order) [authors' own elaboration]

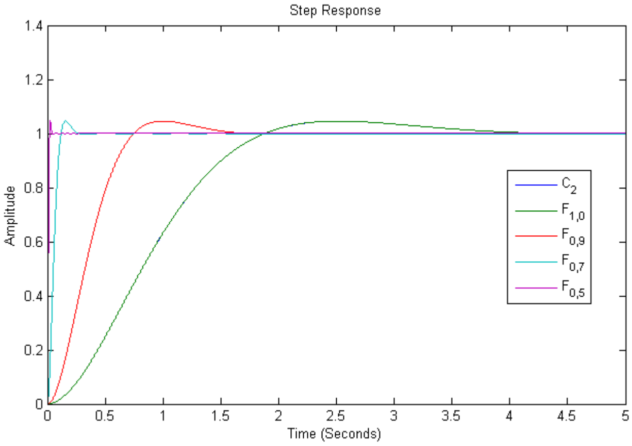

Figure 7. Step response of a pneumatic actuator described with integer and non-integer order: $F_{0,5}$ - for $v=0,5$, $F_{0,7}$ - for $v=0,7$, $F_{0,9}$ - for $v=0,9$, $F_{1,0}$ - for $v=1$, C_2 - classic model (integer order) [authors' own elaboration]

Fig. 6 and Fig. 7 show the impulse and step response described with the formula (19) for selected values v in the interval [0,1]. The impulse and step responses of the tested pneumatic actuator described by means of integer and non-integer differential equations for the parameter $v=1$in the given scale overlap. This indicates the correctness of the analyzed actuator model. Fig. 6 and Fig. 7 show that for increasing values of the orders of the analyzed pneumatic actuator, impulse and step responses behave like the second order oscillatory element. For small orders that converge to 1, the answers behave like the inertial element of the first order.

For the dependence (16) the spectral transfer function of the actuator is obtained:

$$G^{(v)}(j\omega)=\frac{\frac{A}{m}}{(j\omega)^{2v}+\frac{R}{m}(j\omega)^{v}+\frac{C}{m}}$$

$$G^{(v)}(j\omega)=\frac{\frac{A}{m}}{\omega^{2v}\left[\cos(v\pi)+j\sin(v\pi)\right]+\frac{R}{m}\omega^{v}\left[\cos\left(v\frac{\pi}{2}\right)+j\sin\left(v\frac{\pi}{2}\right)\right]+\frac{C}{m}} \tag{20}$$

By making elementary transformations, the real and imaginary part of the spectral transfer function is calculated, where:

$$P^{(v)}(\omega)=\frac{\frac{A}{m}\omega^{2v}\cos(v\pi)+\frac{AR}{m^2}\omega^{v}\cos\left(\frac{v\pi}{2}\right)+\frac{AC}{m^2}}{\left[\omega^{2v}\cos(v\pi)+\frac{R}{m}\omega^{v}\cos\left(\frac{v\pi}{2}\right)+\frac{C}{m}\right]^2+\left[\omega^{2v}\sin(v\pi)+\frac{R}{m}\sin\left(\frac{v\pi}{2}\right)\right]^2}$$

$$Q^{(v)}(\omega)=\frac{\frac{A}{m}\omega^{2v}\sin(v\pi)+\frac{AR}{m^2}\omega^{v}\sin\left(\frac{v\pi}{2}\right)}{\left[\omega^{2v}\cos(v\pi)+\frac{R}{m}\omega^{v}\cos\left(\frac{v\pi}{2}\right)+\frac{C}{m}\right]^2+\left[\omega^{2v}\sin(v\pi)+\frac{R}{m}\sin\left(\frac{v\pi}{2}\right)\right]^2} \tag{21}$$

Knowing the real and imaginary part of the spectral transfer function of the transducer, we can determine the equation describing the logarithmic amplitude step:

$$L^{(v)}(\omega)=20\log\sqrt{\left[P^{(v)}(\omega)\right]^2+\left[Q^{(v)}(\omega)\right]^2} \tag{22}$$

and the equation describing the logarithmic phase step:

$$\varphi^{(v)}(\omega)=arctg\left[\frac{Q^{(v)}(\omega)}{P^{(v)}(\omega)}\right]=-arctg\left[\frac{\omega^{2v}\sin(v\pi)+\frac{R}{m}\omega^{v}\sin\left(\frac{v\pi}{2}\right)}{\omega^{2v}\cos(v\pi)+\frac{R}{m}\omega^{v}\cos\left(\frac{v\pi}{2}\right)+\frac{C}{m}}\right] \tag{23}$$

Using the written program in the MATLAB environment, simulations of equations (22) and (23) were performed to obtain the frequency logarithmic amplitude and phase responses of the actuator, which are shown in Figure 8 and Figure 9.

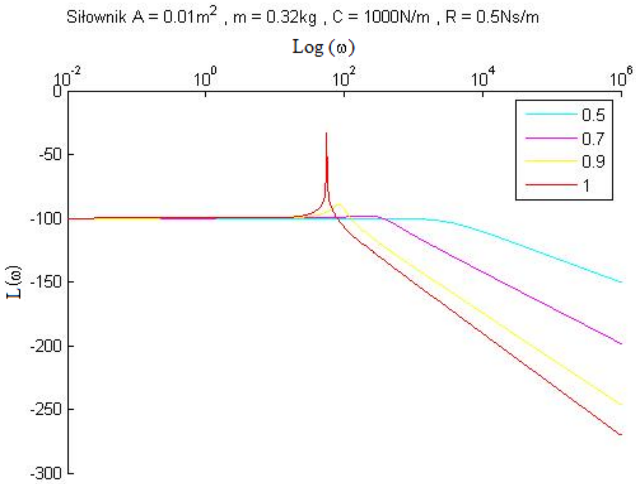

Figure 8. Logarithmic amplitude response of a membrane pneumatic actuator described by means of a differential equation of non-integer orders for different sizes of the parameter v (Siłownik - Pneumatic cylinder) [authors' own elaboration]

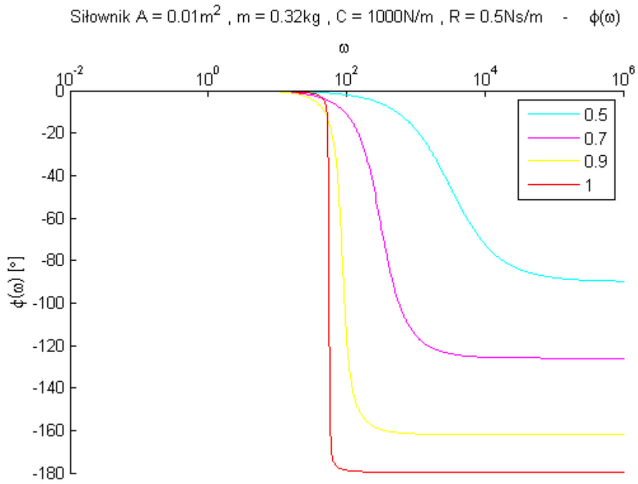

Figure 9. Logarithmic phase response of a pneumatic membrane actuator described by means of a differential equation of non-integer orders for different sizes of the parameter v (Siłownik - Pneumatic cylinder) [authors' own elaboration]

The logarithmic frequency responses (Fig. 8 and Fig. 9) show that for the parameter $v=1$, above the resonant pulsation, the slope of the amplitude response is $-20dB/dek$, as it is in the second order oscillating element. By reducing the order, the gain decreases and the system behaves like the inertial element of the first order.

The course of the logarithmic phase response (Figure 9) confirms this trend. For the parameter $v=1$, the phase response overlaps the logarithmic phase response of the classical second order oscillating element (for the pulsation greater than the resonant one, phase shift reaches the value $\varphi=-\pi$). By reducing the value of the order of the differential, the system becomes the inertial element of the first order, because for the pulsation greater than the resonant one, phase shift decreases. For the parameter $v=0,5$, the phase shift will reach the value $\varphi=-\pi/2$, as it is in the case of the inertial element of the first order.

4 SUMMARY

The obtained responses, which arose from the simulation of the dependencies resulting from the solution of differential equations of integer orders, overlap the responses of non-integer orders obtained from the solution of differential equations of non-integer order for the parameter $v=1$. This is confirmed by the fact that the classical differential calculus is a special case of the differential calculus of any arbitrary order, and thus it proves that mathematical models have been properly developed.

The use of the description of dynamic properties of pneumatic systems based on the fractional calculus will allow the authors of the article to analyze the properties of a wide class of pneumatic systems of arbitrary orders in the future.

BIBLIOGRAPHY

[1] Busłowicz M., Wybrane zagadnienia z zakresu liniowych ciągłych układów niecałkowitego rzędu, Pomiary Automatyka Robotyka nr 2/2010. (in Polish)

[2] Busłowicz M., Nartowicz T., Projektowanie regulatora ułamkowego rzędu dla określonej klasy obiektów z opóźnieniem, Pomiary Automatyka Robotyka, nr 2, s. 398-405, 2009. (in Polish)

[3] Kaczorek T., Wybrane zagadnienia teorii układów niecałkowitego rzędu, Oficyna Wydawnicza Politechniki Białostockiej, stron 271, ISSN 0867-096X, Białystok 2009. (in Polish)

[4] Chwaleba A., Luft M., Właściwości i projektowanie wybranych przetworników mechano–elektrycznych, Zakład Poligraficzny Politechniki Radomskiej, Wyd. II popr. i uzup., ISBN 83-88001-00-0, Radom 1998. (in Polish)

[5] Luft M., Nowocień A., Cioć R., Pietruszczak D., Charakterystyki częstotliwościowe modelu przetwornika ciśnienia opisanego równaniem różniczkowym niecałkowitego rzędu, Logistyka nr 3/2015, ISSN 1231-5478, Poznań 2015. (in Polish)

[6] Luft M., Nowocień A., Pietruszczak D., Analiza właściwości dynamicznych wybranych układów pneumatycznych za pomocą rachunku różniczkowego niecałkowitych rzędów. Część 1. Badania symulacyjne, AUTOBUSY - Technika, Eksploatacja, Systemy Transportowe; Eksploatacja i testy; ISSN 1509-5878, e-ISSN 2450-7725, str. 1050-1055, Instytut Naukowo-Wydawniczy "SPATIUM", AUTOBUSY 12(2017), Radom 2017. (in Polish)

[7] Luft M., Nowocień A., Pietruszczak D., Właściwości dynamiczne wybranych podstawowych członów automatyki niecałkowitych rzędów, AUTOBUSY - Technika, Eksploatacja, Systemy Transportowe; Eksploatacja i testy; ISSN 1509-5878, e-ISSN 2450-7725, str. 1056-1060, Instytut Naukowo-Wydawniczy "SPATIUM", AUTOBUSY 12(2018), Radom 2018. (in Polish)

[8] Luft M., Nowocień A., Pietruszczak D., Analiza właściwości dynamicznych wybranych układów pneumatycznych za pomocą rachunku różniczkowego niecałkowitych rzędów. Część 2. Badania laboratoryjne, AUTOBUSY - Technika, Eksploatacja, Systemy Transportowe; Eksploatacja i testy; ISSN 1509-5878, e-ISSN 2450-7725, str. 1056-1060, Instytut Naukowo-Wydawniczy "SPATIUM", AUTOBUSY 12(2017), Radom 2017. (in Polish)

[9] Luft M., Pietruszczak D., Nowocień A., Frequency response of the pressure transducer model described by the fractional order differential equation, TTS 12 (2016), ISSN 1232-3829, Radom 2016.

[10] Luft M., Szychta E., Nowocień A., Pietruszczak D., Zastosowanie rachunku różniczkowo – całkowego niecałkowitych rzędów w matematycznym modelowaniu przetwornika ciśnienia, Autobusy nr 6/2016, ISSN 1509-5878, Instytut Naukowo-Wydawniczy SPATIUM, Radom 2016 (in Polish)

[11] Nowocień A., Analiza właściwości dynamicznych układów pneumatycznych za pomocą rachunku różniczkowego niecałkowitych rzędów, Rozprawa doktorska, Biblioteka Główna Uniwersytetu Technologiczno- Humanistycznego im. Kazimierza Pułaskiego w Radomiu, Radom 2017, (Promotor: Prof. dr hab. Inż. Mirosław Luft; Promotor pomocniczy: dr inż. Daniel Pietruszczak (in Polish)

[12] Nowocień A., Luft M., Pietruszczak D., Zastosowanie rachunku różniczkowo – całkowego niecałkowitych rzędów w nauce i technice. Logistyka nr 3/2014. (in Polish)

[13] Ostalczyk P., Zarys rachunku różniczkowo-całkowego ułamkowych rzędów. Teoria i zastosowanie w automatyce, Wydawnictwo Politechniki Łódzkiej, stron 430, ISBN 978-83-7283-245-0, Łódź 2008. (in Polish)

[14] Pietruszczak D., Analiza właściwości układów pomiarowych wielkości dynamicznych z wykorzystaniem rachunku różniczkowo – całkowego ułamkowych rzędów, Rozprawa doktorska, Biblioteka Główna Uniwersytetu Technologiczno-Humanistycznego im. Kazimierza Pułaskiego w Radomiu, Radom 2013. (in Polish)

[15] Podlubny I., Fractional Differential Equations. An Introduction to Fractional Derivatives, Fractional Differential Equations, Some Methods of Their Solution and Some of Their Applications, Academic Press, 368 pages, ISBN 0125588402, San Diego-Boston-New York-London-Tokyo-Toronto 1999.

[16] Mościński J., Ogonowski Z. (red.), Advanced Control with MATLAB and SIMULINK, Pearson Higher Education, 272 pages, ISBN 013309667X, 1995.

[17] Rudra P., (tłumacz: Korbecki M.), Matalb 7 dla naukowców i inżynierów, Wydawnictwo Naukowe PWN, stron 280, ISBN 9788301160579, Warszawa 2010.

[18] http://www.mathworks.com – strona internetowa producenta programu MATLAB